

Vibration and acoustic response of an orthotropic composite laminated plate in a hygroscopic environment

Xin Zhao, Qian Geng, and Yueming Li^{a)}

State Key Laboratory for Strength and Vibration of Mechanical Structures, Xi'an Jiaotong University, Xi'an, 710049, People's Republic of China

(Received 4 June 2012; revised 30 November 2012; accepted 22 January 2013)

This paper is a study of the vibration and acoustic response characteristics of orthotropic laminated composite plate with simple supported boundary conditions excited by a harmonic concentrated force in a hygroscopic environment. First the natural vibration of the plate with the in-plane forces induced by hygroscopic stress is obtained analytically. Secondly, the sound pressure distribution of the plate at the far field is obtained using the Rayleigh integral. Furthermore, the sound radiation efficiency is deduced. Third, different ratios of elastic modulus in material principal directions are set to research the effects of increasing stiffness of the orthotropic plate on the vibration and acoustic radiation characteristics. Finally, to verify the theoretical solution, numerical simulations are also carried out with commercial finite software. It is found that the natural frequencies decrease with the increase of the moisture content and the first two order modes interconvert at high moisture content. The dynamic response and sound pressure level float to lower frequencies with elevated moisture content. Acoustic radiation efficiency generally floats to the low frequencies and decreases with an increase of moisture content. The dynamic and acoustic responses reduce and the coincidence frequency decreases with the enhanced stiffness.

© 2013 Acoustical Society of America. [<http://dx.doi.org/10.1121/1.4790353>]

PACS number(s): 43.40.Dx, 43.40.Rj [KML]

Pages: 1433–1442

I. INTRODUCTION

Fiber-reinforced composite structures are extensively used in aerospace, automobile, ship-building industries, and other engineering applications due to their high ratio of strength and stiffness to weight. Composite structures are typically exposed to moist environments in their service life, especially in long-term storage periods. Therefore, the matrix is more susceptible to the hygroscopic condition than the fiber and the deformation is observed to be more in the transverse direction of the composite. Hygroscopic stresses due to the moisture absorbed during the long-term storage period may induce buckling and dynamic instability in structures. The pre-stress effect of hygroscopic load will affect the dynamic behavior of the structure due to the change in stiffness, and then the acoustic characteristics of the structure will be influenced.

Up to now, a lot of work has been done on the dynamic response or acoustic response of a plate under initial in-plane forces. Dickinson¹ researched the free lateral vibrations of simply supported rectangular plates subjected to both direct and shear in-plane forces. Soni and Amba Rao² studied transverse vibrations of orthotropic rectangular plates in the presence of in-plane forces on the basis of classical theory of plates. Qin and Wang^{3,4} analytically studied the dynamic response of a fully clamped metallic sandwich beam under impulsive loading and the dynamic

large deflection response of fully clamped metal foam core sandwich beams struck by a low-velocity heavy mass. Berry *et al.*⁵ analyzed the radiation of sound from a baffled, rectangular plate with the edges elastically restrained against deflection and rotation. It was found that low deflection stiffness at the edges decreases the radiation efficiency of the elastic modes in a spectacular manner. Nelisse *et al.*⁶ studied the radiation of both baffled and unbaffled plates. The Rayleigh–Ritz approach was used to develop the plate displacement in the baffled case, as well as the pressure jump in the unbaffled case. The radiation efficiency of an unbaffled clamped plate in water was presented up to moderate frequencies and compared with that of the baffled plate. Jeyaraj *et al.*^{7,8} adopted commercial finite element software to study the vibration and acoustic response characteristics of an isotropic rectangular plate and a composite plate by considering the inherent material damping property in a thermal environment. Shuyu⁹ studied the far field acoustic pressure distribution of a rectangular radiator analytically and computed the near acoustic field of the radiator numerically. Won *et al.*¹⁰ gave a simple but exact method of calculating the natural frequencies of vibration for some orthotropic laminates with all edges simply supported and under lateral loading and in-plane loading. Ram and Sinha¹¹ investigated the effects of moisture and temperature on the free vibration of laminated composite plates. The analysis was carried out by the finite element method and also accounted for lamina material properties at elevated moisture content and temperature. The results showed a reduction in the natural frequency with the increase of the uniform moisture content and temperature.

^{a)}Author to whom correspondence should be addressed. Electronic mail: liyueming@mail.xjtu.edu.cn

Parhi *et al.*¹² studied the free vibration and transient response of multiple delaminated doubly curved composite shells subjected to a hygrothermal environment with a finite element formulation based on the first order shear deformation theory. Naidu and Sinha^{13–15} investigated the nonlinear transient response and nonlinear free vibration behavior of laminated composite shells subjected to hygrothermal environments using the finite element method. The parametric study was carried out by varying the curvature ratios and side to thickness ratios of composite cylindrical, spherical, and hyperbolic parabolic shell panels with simply supported boundary conditions. Lyrantzis and Bofilios¹⁶ presented an analytical study to predict dynamic response and noise transmission of discretely stiffened multi-layered composite panels and examined the effects of the temperature and high humidity. Geng and Li¹⁷ studied the vibration and acoustic radiation characteristics of a thermally stressed plate theoretically. Numerical methods were also employed to validate the results. They found that the natural frequencies of the plate reduce with temperature rise and the response curves float to lower frequency range. The radiation efficiency of the plate reduces quite evidently below and above the critical frequency.

However, there are few studies available in the literature with respect to vibration and acoustic response of an orthotropic composite plate in a hygroscopic environment. In this paper, the vibration and acoustic response of an orthotropic laminated composite plate in a hygroscopic environment subjected to steady state excitations are investigated analytically. The effect of the moisture content on the natural frequencies for the plate is investigated. The sound pressure level and sound radiation efficiency of the plate under hygroscopic stress at the far field are obtained. The different ratios of the two elastic moduli in material principal directions, namely, the ratios of the longitudinal tensile modulus to the transverse tensile modulus, are assigned artificially to research the effects of different stiffness values of the orthotropic plate at moisture content on vibration and acoustic response characteristics. To compare with the theoretical solution, numerical simulations are also carried out by commercial finite element software.

II. MATHEMATICAL MODEL

A hypothesis is given that the orthotropic rectangular thin plate radiator under a hygroscopic environment in vibration is mounted on a flat rigid baffle of infinite extent. The Cartesian coordinates are sketched in Fig. 1. The dimensions of the plate are a in the x direction, b in the y direction, and h thickness. Radiation is considered only into the half-space defined by $+z$. The acoustic pressure at the field point P can be obtained by dividing the radiating surface of the plate into infinitesimal elements, each of which acts like a baffled simple source of strength.

A laminate composed of N layer laminas is considered. All lamina are orthotropic containing three planes of

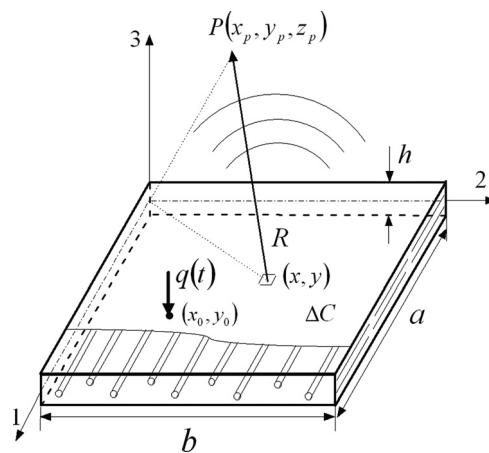


FIG. 1. A rectangular orthotropic composite plate in vibration and its coordinates.

elastic symmetry and the material principal directions are coincident with the coordinate system (x, y) , so laminate bonding together with the lamina having the same principal coordinate system can be assumed for the orthotropic laminate plate. In the present study, based on the Kirchhoff hypothesis, classical plate theory will be adopted in the analysis.

A. In-plane force induced by hygroscopic stress

Assume that the plate is stress free at the reference moisture content $C_i(\%)$. When the structure moisture content changes to $C_f(\%)$, the stress state of the plate will be changed by the resulting hygroscopic stresses. If the moisture content change across the thickness is uniform, the plate can be described with the plane stress state. The stress-displacement relations will be^{18,19}

$$\begin{aligned}\sigma_1 &= \frac{E_1}{1 - \nu_{12}\nu_{21}} \left[\left(\frac{\partial u_0}{\partial x} + \nu_{21} \frac{\partial v_0}{\partial y} \right) - (\beta_1 + \nu_{21}\beta_2)\Delta C \right], \\ \sigma_2 &= \frac{E_2}{1 - \nu_{12}\nu_{21}} \left[\left(\frac{\partial v_0}{\partial y} + \nu_{12} \frac{\partial u_0}{\partial x} \right) - (\beta_2 + \nu_{12}\beta_1)\Delta C \right], \\ \tau_{12} &= G_{12} \left(\frac{\partial u_0}{\partial y} + \frac{\partial v_0}{\partial x} \right),\end{aligned}\quad (1)$$

where u_0 and v_0 are the in-plane displacements, E_1 and E_2 are the longitudinal Young's modulus (in direction 1) and transverse Young's modulus (in direction 2), respectively, G_{12} is the shear modulus, ν_{12} and ν_{21} are Poisson's ratios, β_1 and β_2 are the longitudinal and transverse coefficients of hygroscopic expansion, and $\Delta C(\%) = C_f - C_i$ is denoted as the moisture content change.

The distribution of stress along the thickness of the plate can be expressed by the resultant forces and moments at the middle surface. The distribution of moisture content in the plate is assumed to be uniform. Integrating Eqs. (1) along the thickness of the plate yields

$$\begin{aligned}
N_x &= \int_{-h/2}^{h/2} \sigma_1 dz = \int_{-h/2}^{h/2} \frac{E_1}{1 - \nu_{12}\nu_{21}} \left(\frac{\partial u_0}{\partial x} + \nu_{21} \frac{\partial v_0}{\partial y} \right) dz \\
&\quad - \frac{E_1(\beta_1 + \nu_{21}\beta_2) \int_{-h/2}^{h/2} \Delta C dz}{1 - \nu_{12}\nu_{21}} \\
&= \frac{E_1 h}{1 - \nu_{12}\nu_{21}} \left(\frac{\partial u_0}{\partial x} + \nu_{21} \frac{\partial v_0}{\partial y} \right) - \frac{E_1(\beta_1 + \nu_{21}\beta_2) \Delta C h}{1 - \nu_{12}\nu_{21}}, \\
N_y &= \int_{-h/2}^{h/2} \sigma_2 dz = \int_{-h/2}^{h/2} \frac{E_2}{1 - \nu_{12}\nu_{21}} \left(\frac{\partial v_0}{\partial y} + \nu_{12} \frac{\partial u_0}{\partial x} \right) dz \\
&\quad - \frac{E_2(\beta_2 + \nu_{12}\beta_1) \int_{-h/2}^{h/2} \Delta C dz}{1 - \nu_{12}\nu_{21}} \\
&= \frac{E_2 h}{1 - \nu_{12}\nu_{21}} \left(\frac{\partial v_0}{\partial y} + \nu_{12} \frac{\partial u_0}{\partial x} \right) - \frac{E_2(\beta_2 + \nu_{12}\beta_1) \Delta C h}{1 - \nu_{12}\nu_{21}}, \\
N_{xy} &= \int_{-h/2}^{h/2} \tau_{12} dz = G_{12} h \left(\frac{\partial u_0}{\partial y} + \frac{\partial v_0}{\partial x} \right). \tag{2}
\end{aligned}$$

In the present study, the hygroscopic environment is assumed to induce a uniform plane-wise moisture content rise in the plate. Taking the boundary condition into account, the hygroscopic load here will not cause in-plane displacement, so Eq. (2) will be simplified to

$$\begin{aligned}
N_x &= -\frac{E_1(\beta_1 + \nu_{21}\beta_2) \Delta C h}{1 - \nu_{12}\nu_{21}}, \\
N_y &= -\frac{E_2(\beta_2 + \nu_{12}\beta_1) \Delta C h}{1 - \nu_{12}\nu_{21}}, \\
N_{xy} &= 0. \tag{3}
\end{aligned}$$

B. Vibration of the plate in a hygroscopic environment

The Lagrangian differential equation in the usual notation for small amplitude vibrations of uniform orthotropic rectangular plates excited by a harmonic concentrated force on an arbitrary point on the surface of the plates, in the presence of in-plane forces, is given by^{1,2}

$$\begin{aligned}
D_1 \frac{\partial^4 w}{\partial x^4} + 2D_3 \frac{\partial^4 w}{\partial x^2 \partial y^2} + D_2 \frac{\partial^4 w}{\partial y^4} + \rho \frac{\partial^2 w}{\partial t^2} \\
= N_x \frac{\partial^2 w}{\partial x^2} + N_y \frac{\partial^2 w}{\partial y^2} + 2N_{xy} \frac{\partial^2 w}{\partial x \partial y} + q, \tag{4}
\end{aligned}$$

where

$$\begin{aligned}
D_1 &= \frac{E_1(1 + \eta_{1j})h^3}{12(1 - \nu_{12}\nu_{21})}, \\
D_2 &= \frac{E_2(1 + \eta_{2j})h^3}{12(1 - \nu_{12}\nu_{21})}, \\
D_3 &= D_1\nu_{21} + \frac{G_{12}(1 + \eta_{12j})h^3}{6}, \tag{5}
\end{aligned}$$

$$q = q_0 \delta(x - x_0, y - y_0) e^{j\omega t}. \tag{6}$$

D_1 , D_2 , and D_3 are the flexural rigidity of plate; η_1 , η_2 are loss factors in the principal direction and η_{12} is the loss factor in the shear direction; h is the thickness of the plate; q is the harmonic concentrated excitation force on point (x_0, y_0) ; and j is the imaginary unit.

According to Eq. (4), the equation of motion of the orthotropic plate in a hygroscopic environment can be expressed by^{2,16}

$$\begin{aligned}
D_1 \frac{\partial^4 w}{\partial x^4} + 2D_3 \frac{\partial^4 w}{\partial x^2 \partial y^2} + D_2 \frac{\partial^4 w}{\partial y^4} + (1 + \Delta C) \rho h \frac{\partial^2 w}{\partial t^2} \\
= N_x \frac{\partial^2 w}{\partial x^2} + N_y \frac{\partial^2 w}{\partial y^2} + 2N_{xy} \frac{\partial^2 w}{\partial x \partial y} + q \tag{7}
\end{aligned}$$

and the factor $(1 + \Delta C)$ in front of the mass of the plate accounts for the absorbed moisture.

With the boundary conditions, four edges of the plate $x = 0$, $x = a$, $y = 0$, $y = b$ are simply supported. Let us expand the displacement in a series of the plate modes:¹⁷

$$w(x, y, t) = \sum_{m,n} W_{mn} \phi_{mn}(x, y) e^{j\omega t}, \tag{8}$$

where m and n are modal indices, W_{mn} is the amplitude of mode displacement, and $\phi_{mn}(x, y)$ is the mode shape function for simple supported boundary conditions given by

$$\phi_{mn}(x, y) = \sin \frac{m\pi x}{a} \sin \frac{n\pi y}{b}. \tag{9}$$

To find the vibration response of the preloaded structure, the weighted residual (Galerkin) method is used to solve the Eq. (7), and the integral of a weight residual of mode shape function should be set to zero. So we can obtain

$$\begin{aligned}
\iint_{\Omega} \left[D_1 \frac{\partial^4 w}{\partial x^4} + 2D_3 \frac{\partial^4 w}{\partial x^2 \partial y^2} + D_2 \frac{\partial^4 w}{\partial y^4} + (1 + \Delta C) \rho h \frac{\partial^2 w}{\partial t^2} \right. \\
\left. - \left(N_x \frac{\partial^2 w}{\partial x^2} + N_y \frac{\partial^2 w}{\partial y^2} + 2N_{xy} \frac{\partial^2 w}{\partial x \partial y} \right) - q \right] \phi_{kl}(x, y) dA = 0. \tag{10}
\end{aligned}$$

Substituting Eqs. (3), (8), and (9) into Eq. (10), and using the orthogonality properties of the mode shape gives

$$\begin{aligned}
\iint_{\Omega} \left[\left(D_1 \frac{\partial^4}{\partial x^4} \phi_{mn}(x, y) + 2D_3 \frac{\partial^4}{\partial x^2 \partial y^2} \phi_{mn}(x, y) \right. \right. \\
\left. \left. + D_2 \frac{\partial^4}{\partial y^4} \phi_{mn}(x, y) \right) \phi_{kl}(x, y) \right. \\
\left. - \left(N_x \frac{\partial^2 w}{\partial x^2} + N_y \frac{\partial^2 w}{\partial y^2} + 2N_{xy} \frac{\partial^2 w}{\partial x \partial y} \right) \phi_{kl}(x, y) \right] dA \\
= \omega_{mn}^2 \iint_{\Omega} (1 + \Delta C) \rho h \phi_{mn}(x, y) \phi_{kl}(x, y) dA \\
= \begin{cases} \omega_{mn}^2 & m = k \text{ and } n = l \\ 0 & m \neq k \text{ or } n \neq l. \end{cases} \tag{11}
\end{aligned}$$

The amplitude of mode displacement can be expressed as

$$W_{mn} = \frac{Q_{mn}}{\omega_{mn}^2 - \omega^2}, \quad (12)$$

where $Q_{mn} = q_0 \sin(m\pi x_0/a) \sin(n\pi y_0/b)$ is the orthogonalized force, ω is the frequency of applied load, and ω_{mn} is the natural frequency of the (m, n) mode:

$$\omega_{mn}^2 = \frac{\pi^2}{(1 + \Delta C)\rho h} \left\{ \pi^2 \left[D_1 \left(\frac{m}{a}\right)^4 + 2D_3 \left(\frac{m}{a}\right)^2 \left(\frac{n}{b}\right)^2 + D_2 \left(\frac{n}{b}\right)^4 \right] + N_x \left(\frac{m}{a}\right)^2 + N_y \left(\frac{n}{b}\right)^2 \right\}. \quad (13)$$

Therefore, under the excitation of a harmonic concentrated force, the displacement of the plate in a hygroscopic environment can be obtained as

$$w(x, y, t) = \sum_{m,n} \frac{Q_{mn}}{\omega_{mn}^2 - \omega^2} \sin \frac{m\pi x}{a} \sin \frac{n\pi y}{b} e^{j\omega t} \quad (14)$$

and the velocity of the plate can be deduced as

$$v(x, y, t) = \sum_{m,n} V_{mn} \phi_{mn}(x, y) e^{j\omega t}, \quad (15)$$

where V_{mn} is the complex amplitude of mode velocity of the (m, n) mode and can be expressed by

$$V_{mn} = \frac{j\omega Q_{mn}}{\omega_{mn}^2 - \omega^2}. \quad (16)$$

C. Calculation for critical buckling moisture content

The effect of hygroscopic environments is assumed to change the plate moisture content uniformly in both plane-wise and thickness directions. The entire hygroscopic load cases are designed below the critical buckling moisture content. The critical buckling load of plates compressed in two perpendicular directions and the differential equation for the elastic stability of the orthotropic plate with a simply supported boundary condition can be written

$$D_1 \frac{\partial^4 w}{\partial x^4} + 2D_3 \frac{\partial^4 w}{\partial x^2 \partial y^2} + D_2 \frac{\partial^4 w}{\partial y^4} = N_x \frac{\partial^2 w}{\partial x^2} + N_y \frac{\partial^2 w}{\partial y^2}. \quad (17)$$

Assume that the elastic surface equation after buckling is

$$w = A_{mn} \sin \frac{m\pi x}{a} \sin \frac{n\pi y}{b}. \quad (18)$$

Inserting Eq. (18) into (17), one can obtain the equation

$$\pi^4 \times \left[D_1 \left(\frac{m}{a}\right)^4 + 2D_3 \left(\frac{mn}{ab}\right)^2 + D_2 \left(\frac{n}{b}\right)^4 \right] + N_x \left(\frac{\pi m}{a}\right)^2 + N_y \left(\frac{\pi n}{b}\right)^2 = 0. \quad (19)$$

Substituting Eq. (3) into Eq. (19), the expression for critical buckling moisture content C_{cr} (%) can be obtained:

$$C_{cr} = \frac{\pi^2 \left[D_1 \left(\frac{m}{a}\right)^4 + 2D_3 \left(\frac{mn}{ab}\right)^2 + D_2 \left(\frac{n}{b}\right)^4 \right]}{\frac{h}{1 - \nu_{12}\nu_{21}} \left[E_1 (\beta_1 + \nu_{21}\beta_2) \left(\frac{m}{a}\right)^2 + E_2 (\beta_2 + \nu_{12}\beta_1) \left(\frac{n}{b}\right)^2 \right]}. \quad (20)$$

As the variables m and n take proper values, the minimum value obtained from Eq. (20) is the critical buckling moisture content.

D. Radiation acoustic field of the plate

Based on the Rayleigh integral, the sound pressure distribution of the radiator at point $P(x_p, y_p, z_p)$ in the far field is given by²⁰

$$p(x_p, y_p, z_p, t) = \frac{j\omega\rho_0}{2\pi} e^{j\omega t} \int_s \frac{\sum_{mn} V_{mn} \phi_{mn}(x, y) e^{-jkR}}{R} ds, \quad (21)$$

where ρ_0 is the density of air, $k = \omega/c_0$ is the wave number, c_0 is the speed of sound in air, $s = ab$, and $R = \sqrt{(x_p - x)^2 + (y_p - y)^2 + z_p^2}$ is the distance between

the observation point (x_p, y_p, z_p) in the acoustic field and the integration point (x, y) on the plate.

The time-averaged sound power radiation can be evaluated by integrating the product of the surface sound pressure, $p(x, y, 0, t)$, and the transverse velocity of the plate, $v(x, y, t)$, over the surface of a panel. for harmonic vibration,

$$\bar{\Pi}(\omega) = \frac{1}{2} \int_0^a \int_0^b \text{Re}[\tilde{v}_n(x, y, \omega)^* \tilde{p}(x, y, 0, \omega)] dx dy, \quad (22)$$

where the asterisk denotes complex conjugate. Then the sound radiation efficiency obtained from the sound power is defined as

$$\bar{\sigma} = \frac{\bar{\Pi}}{\rho_0 c_0 s \langle \bar{v}^2 \rangle}, \quad (23)$$

where $\langle \bar{v}^2 \rangle = (1/2s) \int_s |v|^2 ds$ is the temporal and spatial average of the square of the surface velocity of the plate.

TABLE I. Elastic module of carbon-epoxy lamina at different moisture contents.

Elastic Modulus (GPa)	Moisture content, ΔC (%)						
	0.0	0.25	0.50	0.75	1.00	1.25	1.50
E_1	172.5	172.5	172.5	172.5	172.5	172.5	172.5
E_2	6.90	6.72	6.54	6.36	6.17	6.17	6.17
G_{12}	3.45	3.45	3.45	3.45	3.45	3.45	3.45

III. RESULTS AND DISCUSSION

In this section, the vibration response and acoustic radiation characteristics for the orthotropic plate excited by a harmonic concentrated force will be discussed by assuming that the structure is subjected to a uniform moisture content rise. On the one hand, the critical buckling moisture content as a parameter and the vibration response and acoustic radiation characteristics for the plate at elevated moisture content are researched. The analysis accounts for lamina material properties at elevated moisture content. On the other hand, to research the effects of different stiffness values on the vibration response and acoustic radiation characteristics for the plate at certain moisture contents, different ratios for the longitudinal Young's modulus to the transverse Young's modulus will be assigned artificially.

A rectangular orthotropic composite laminated plate with dimensions $0.4 \times 0.3 \times 0.01 \text{ m}^3$ which is excited at $(a/4, b/4, 0)$ by harmonic excitation with amplitude 1N in the normal direction is now considered for a detailed investigation. The mechanical properties for the carbon-epoxy composites are assumed to be as follows:¹² $E_1 = 172.5 \text{ GPa}$, $E_2 = 6.9 \text{ GPa}$, $G_{12} = G_{13} = 3.45 \text{ GPa}$, $\rho = 1600 \text{ kg/m}^3$, $\nu_{12} = 0.25$, $\eta_1 = 0.0007$, $\eta_2 = 0.0067$, $\eta_{12} = 0.0112$, $\beta_1 = 0$, and $\beta_2 = 0.44$.

The lamina material properties at the elevated moisture contents used in the present analysis are shown in Table I.¹² The density of the air (acoustic medium) and the velocity of the sound are assumed to be $\rho_0 = 1.21 \text{ kg/m}^3$, $c_0 = 343.0 \text{ m/s}$.

A. Vibration and acoustic responses of the plate at elevated moisture contents

The vibration and acoustic responses of the plate in a hygroscopic environment for simply supported boundary conditions have been studied by assuming that the structure is subjected to a uniform moisture content rise. All the hygroscopic load cases are designed below the critical buckling moisture content. According to Sec. II C and substituting the parameters in Eq. (20), the critical buckling moisture content $C_{cr} = 1.48\%$ can be obtained as $m = 1$, $n = 2$. Therefore, four load cases are chosen with uniform moisture content rises ΔC of 0.37% ($0.25C_{cr}$), 0.74% ($0.5C_{cr}$), 1.11% ($0.75C_{cr}$), and 1.47% ($0.99C_{cr}$), respectively, and 0.0% is defined as the reference moisture content to represent the stress free state case. So according to the lamina material properties at the elevated moisture contents in Table I, the modulus of elasticity for E_2 can be converted into 6.63,

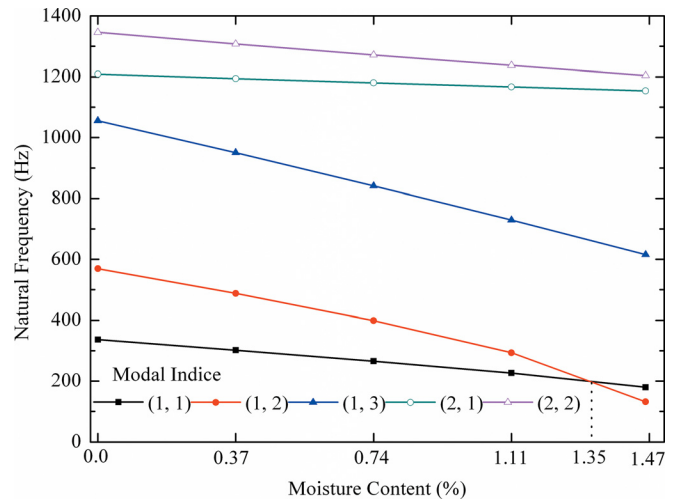


FIG. 2. (Color online) Effects of moisture content on the natural frequency of the orthotropic composite plate.

6.36, 6.17, and 6.17 GPa corresponding with the moisture contents 0.37%, 0.74%, 1.11%, and 1.47%.

First, the pre-stressed modal analysis is carried out for elevated uniform moisture contents ΔC in the plate from 0.0%, 0.37%, 0.74%, 1.11%, to 1.47% for simply supported boundary conditions to find the influence of hygroscopic environment on natural frequencies and corresponding mode shapes. The results obtained from the pre-stressed modal analysis are given in Fig. 2 and Table II which shows the lowest five natural frequencies for various values of moisture content rise; the modal indices are stated in brackets. It is seen that the natural frequency generally decreases with an increase in uniform moisture content. In Table II one can see the modal indices stay the same in SI Nos. (solution numbers) 3, 4, and 5 modes with moisture content rise, and the modal indices of SI Nos. 1 and 2 remain unchanged from 0.0% to 1.11% moisture contents but interconvert at 1.47% moisture content. It is more obvious in Fig. 2 that the curves of (1, 1) and (1, 2) modes intersect at 1.35% moisture content and the modal indices of SI No. 1 transform from (1, 1) into (1, 2) while those of SI No. 2 transform from (1, 2) into (1, 1). Therefore, the natural frequency of the (1, 2) mode will be less than the (1, 1) mode when the moisture content is greater than 1.35%. The frequency ratios, defined by $\lambda = f_C/f_0$ are plotted in Fig. 3, where f_C and f_0 are the natural frequencies of each mode shape obtained with hygroscopic loads and under the reference moisture content (0.0% in this work). The absolute value of the slope of frequency ratio curve of the

TABLE II. Natural frequencies for simply supported orthotropic plate with hygroscopic loads (Hz).

SI No.	Hygroscopic loads				
	0.0%	0.37%	0.74%	1.11%	1.47%
1	336.4(1,1)	301.4(1,1)	265.4(1,1)	226.5(1,1)	131.7(1,2)
2	569.2(1,2)	487.8(1,2)	398.6(1,2)	293.3(1,2)	179.6(1,1)
3	1055.6(1,3)	950.5(1,3)	841.3(1,3)	729.4(1,3)	615.6(1,3)
4	1209.0(2,1)	1194.1(2,1)	11802(2,1)	1166.9(2,1)	1153.7(2,1)
5	1345.8(2,2)	1307.7(2,2)	1271.5(2,2)	1237.2(2,2)	1204.1(2,2)

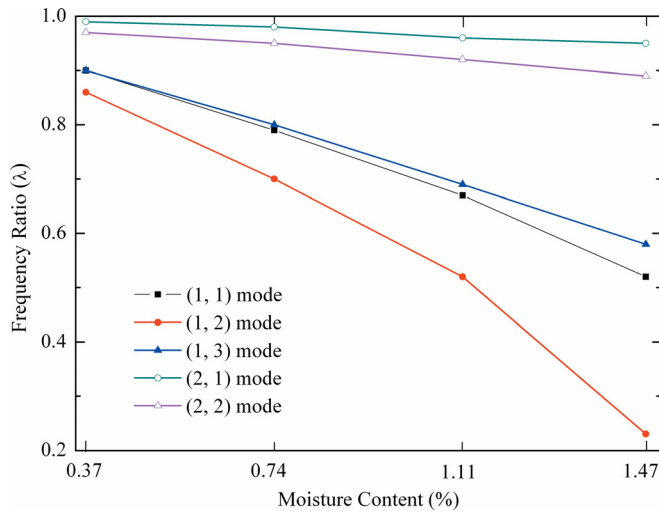


FIG. 3. (Color online) Frequency ratio for the first five natural frequencies.

(1, 2) mode is much greater than others, and the slope increases more rapidly with the moisture content rise. The reason for this is that the elastic modulus in principle direction 2 of the material is far less than that in principle direction 1 in our work, and the reduction of stiffness due to the elevated moisture content in direction 2 is far more than in direction 1 for the high moisture content, which makes the interconversion of mode shapes of SI Nos. 1 and 2 at high moisture content.

The temporal and spatial averages of the square of surface velocities of the plate in the exciting point are calculated under harmonic excitations under different hygroscopic environments and given in Fig. 4. The velocities reach maximum resonant frequencies given by the curves of different moisture content. For the change of natural vibration under hygroscopic loads, it is clear that the resonances corresponding to structural modes move to lower frequencies as the stiffness reduces.

Figure 5 shows the sound pressure level at the point above the exciting point in 4.0 m of the plate with different moisture content. The plot describes the sound pressure

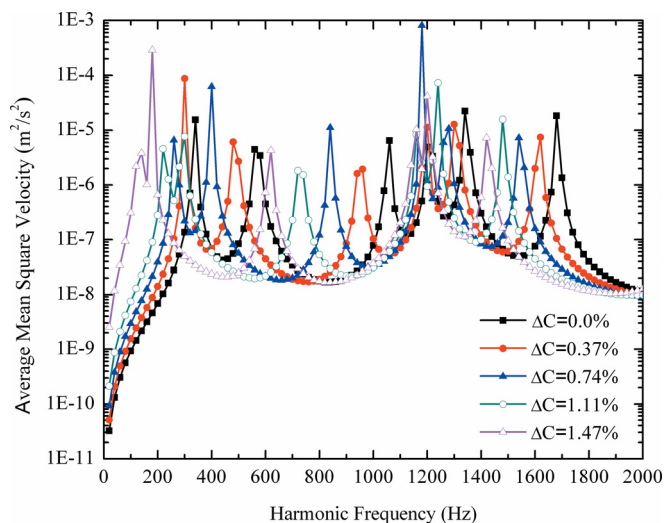


FIG. 4. (Color online) Effects of moisture content on the average mean square velocity of the orthotropic composite plate.

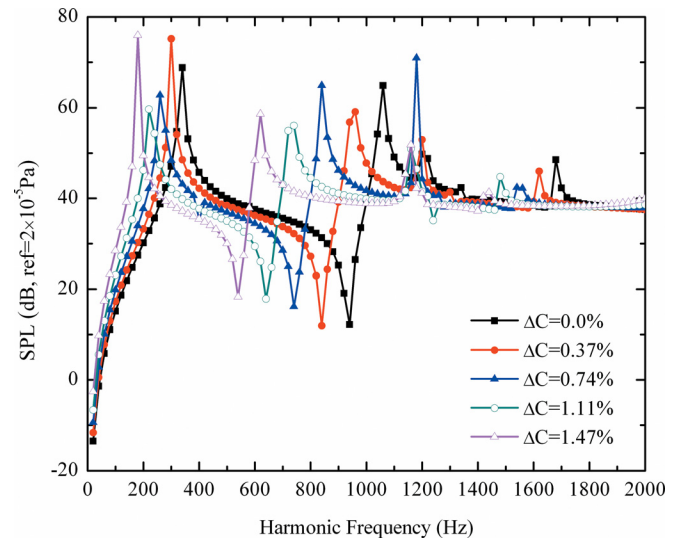


FIG. 5. (Color online) Effects of moisture content on the sound pressure level of the orthotropic composite plate.

level, which appears to shift to low frequencies with the moisture content for the harmonic frequency within the range of 1–2000 Hz. The peaks of sound pressure level appear obviously in (1, 1) and (1, 3) resonance modes with different moisture content but the peaks of the other modes are not obvious. For example, in the plot of the sound pressure level at 0.37% moisture content, one can see the peaks in (1, 1) (301.4 Hz) and (1, 3) (950.5 Hz) modes are more obvious than in (1, 2) (487.8 Hz), (2, 1) (1194.1 Hz), and (2, 2) (1307.7 Hz) modes.

Figure 6 shows the sound radiation efficiency of the orthotropic plate as a function of frequency. In the plot one can see that the radiation efficiency generally floats to the low frequencies and decreases with an increase in moisture content. Orthotropic plates have two coincidence frequencies: one corresponding to bending waves in the longitudinal direction (fiber direction) and another one corresponding to bending waves in the transverse direction. The values of two

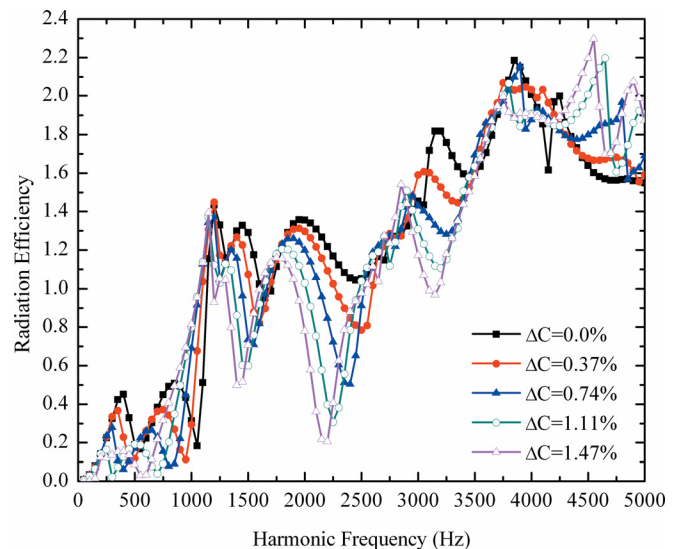


FIG. 6. (Color online) Effects of the moisture content on radiation efficiency of the orthotropic composite plate.

coincidence frequencies were obtained from the analytical expression given by Ohlrich and Hugin.²¹ For the orthotropic plate analyzed in the present work these frequencies are 1220 and 3850 Hz, respectively. Figure 6 shows that radiation efficiency crosses one at the lower coincidence frequency and decreases towards one only after the second coincidence frequency.

B. Effects of different stiffness values on the vibration and acoustic responses of the plate at a moisture content

In this section, to research the effects of different stiffness values on the vibration and acoustic responses of the plate at a moisture content, we keep the longitudinal Young's modulus E_1 unchanged at 172.5 GPa while assuming that transverse Young's modulus E_2 artificially increases from 6.9 to 17.25, 34.5, and 172.5 GPa, so the stiffness of the orthotropic plate increases gradually as the ratio of E_1 to E_2 reduces from 25 to 10, 5, and 1. When the ratio reduces to 1, the orthotropic plate is approximately equivalent to an isotropic plate.

The effects of the different stiffness values on the average mean square velocity of the plate at 0.37% moisture content are shown in Fig. 7. It can be observed that the peaks in resonance modes reduce in the 1–2000 Hz range with the enhancement of the stiffness due to the decreasing ratio of E_1/E_2 .

Figure 8 shows the effects of the different ratios of elastic modulus on the sound pressure level of the plate at 0.37% moisture content. There are many peaks for each curve, and the peaks appear in the resonance frequencies because the acoustic response is influenced by the dynamic response of the plate. As well as the trend in Fig. 7, with the ratio reducing, the stiffness of the plate enhanced and the number of resonance modes reduce in the 1–2000 Hz range, so the number of peaks decreases.

Figure 9 illustrates the effects of the different ratios of E_1 to E_2 on the radiation efficiency for the plate at 0.37% moisture content in the 1–5000 Hz harmonic frequency

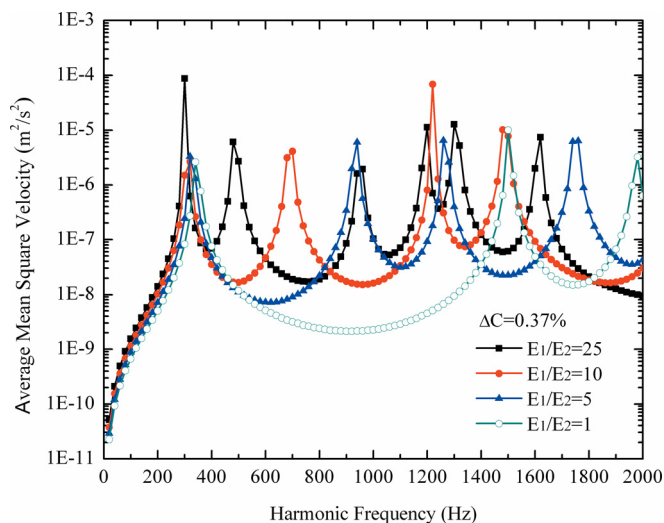


FIG. 7. (Color online) Effects of different stiffness values on average mean square velocity at 0.37% moisture content.

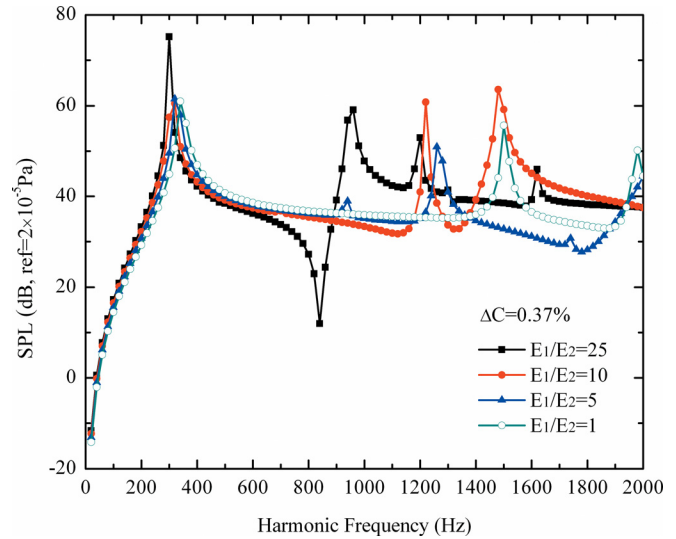


FIG. 8. (Color online) Effects of the different stiffness values on sound pressure level at 0.37% moisture content.

range. It shows the fluctuation of the radiation efficiency decrease with the enhanced stiffness for the decrease of the ratio. For the orthotropic plates having two coincidence frequencies mentioned above, it can be observed that the greater the stiffness, the smaller the second coincidence frequency corresponding to bending waves in the transverse direction. The orthotropic plate is approximately equivalent to an isotropic plate, while the ratio of E_1 to E_2 is equal to 1. The plot shows a clear peak around the coincidence frequency, followed by an asymptotic reduction to unity, as expected.

IV. VALIDATION

The finite element method (FEM) is used to carry out numerical simulations for the same model used in Sec. III A to process a validation study. As is well known, the thermoelastic problem can be resolved by the FEM software

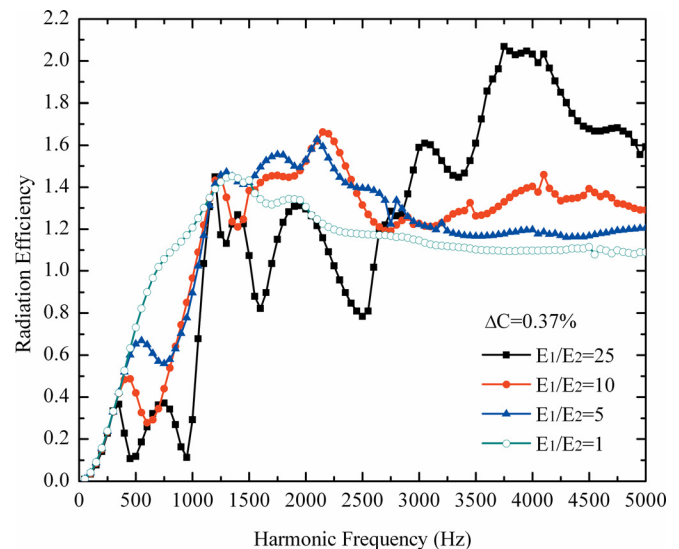


FIG. 9. (Color online) Effects of different stiffness values on radiation efficiency at 0.37% moisture content.

TABLE III. Comparisons of natural frequencies (Hz) of theoretical and numerical results.

SI No.		0.0%	0.37%	0.74%	1.11%	1.47%
1	Theoretical	336.4(1,1)	301.4(1,1)	265.4(1,1)	226.5(1,1)	131.7(1,2)
	MD NASTRAN	335.5(1,1)	300.4(1,1)	264.2(1,1)	225.0(1,1)	124.8(1,2)
	Error (%)	0.27	0.33	0.45	0.66	5.24
2	Theoretical	569.2(1,2)	487.8(1,2)	398.6(1,2)	293.3(1,2)	179.6(1,1)
	MD NASTRAN	568.6(1,2)	486.8(1,2)	397.0(1,2)	290.7(1,2)	177.8(1,1)
	Error (%)	0.11	0.16	0.40	0.89	1.0
3	Theoretical	1055.6(1,3)	950.5(1,3)	841.3(1,3)	729.4(1,3)	615.6(1,3)
	MD NASTRAN	1058.6(1,3)	952.9(1,3)	843.3(1,3)	730.7(1,3)	616.3(1,3)
	Error (%)	0.28	0.25	0.24	0.17	0.11
4	Theoretical	1209.0(2,1)	1194.1(2,1)	1180.2(2,1)	1166.9(2,1)	1153.7(2,1)
	MD NASTRAN	1199.6(2,1)	1184.6(2,1)	1170.6(2,1)	1157.2(2,1)	1143.8(2,1)
	Error (%)	0.78	0.79	0.81	0.83	0.86
5	Theoretical	1345.8(2,2)	1307.7(2,2)	1271.5(2,2)	1237.2(2,2)	1204.1(2,2)
	MD NASTRAN	1335.0(2,2)	1296.6(2,2)	1260.0(2,2)	1225.3(2,2)	1191.7(2,2)
	Error (%)	0.80	0.85	0.90	0.96	1.03

adequately, and because the moisture change leads to swelling strains and stresses similar to those due to thermal expansion, a similar method carried out in a thermoelastic problem in FEM software could be used to resolve the problems with the hygroscopic stress induced in the structures. The strategy adopted to resolve the thermal stress problems will be used to obtain the strains related to the hygroscopic environment in this validation research.

The validation for natural vibration is carried out by finite element software MD NASTRAN. The plate is modeled

using the four-noded quadrilateral structural shell element available in the MD NASTRAN element library. The mesh density of the FEM modal of the plate is 32×32 in MD NASTRAN. To verify the vibration characteristic of the plate between the theoretical solutions and numerical results obtained from MD NASTRAN, the comparisons of natural frequencies are listed in Table III, and the modal indices are in brackets. The error between the theoretical solution and MD NASTRAN is defined by $(|f_i - f_N|/f_i) \times 100\%$, where f_i and f_N are the natural frequencies of the theoretical and numerical solutions, respectively. The first five mode shapes with 0.0, 0.74, and 1.47% moisture contents obtained from MD NASTRAN are presented in Fig. 10. It can be seen that the natural frequencies and mode shapes calculated by the two methods match very well.

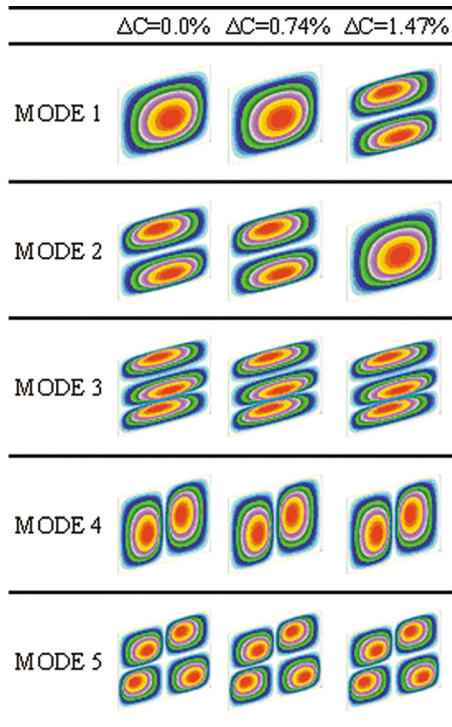


FIG. 10. (Color online) Mode shapes at different values of uniform moisture content rise.

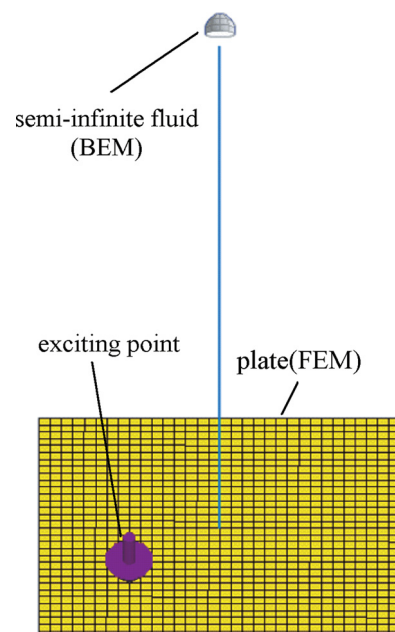


FIG. 11. (Color online) FEM/BEM model of v_a ONE.

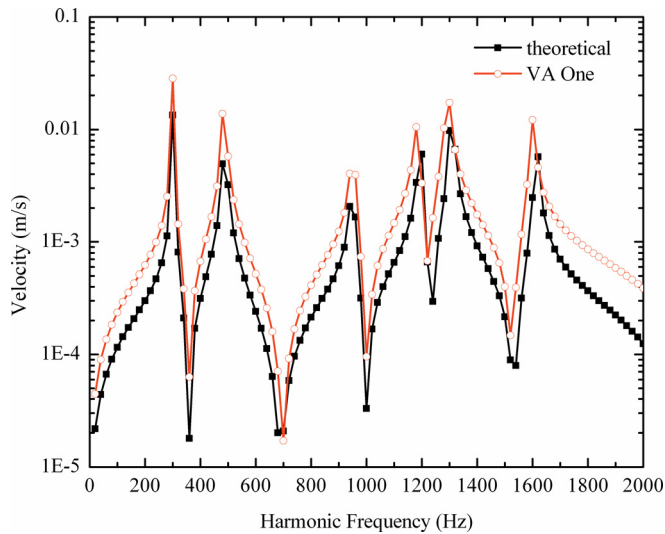


FIG. 12. (Color online) Velocity response comparisons at the excitation point of the plate at 0.37% moisture content.

To make a verification of the vibration and acoustic responses with the theoretical solution, FEM and the boundary element method (BEM) are used to calculate the sound pressure level for the point above the exciting point 4.0 m. In the FEM/BEM analysis, finite element meshes are used to model the plate, while the BEM fluid is used to simulate the acoustic field. Normal mode results are obtained from MD NASTRAN with finite element analysis and imported into the finite element software package VA ONE, and then the structure response and BEM fluid analysis are carried out. Figure 11 is the FEM/BEM model of VA ONE for the calculation of sound pressure level of the plate at 0.37% moisture content.

The velocity response comparison at the harmonic excitation point on the plate at 0.37% moisture content is plotted in Fig. 12. The response curves show good agreement. Because of the difference of natural frequencies between the theoretical values and numerical results, the response peaks appear a little mismatched and the numerical result is a little

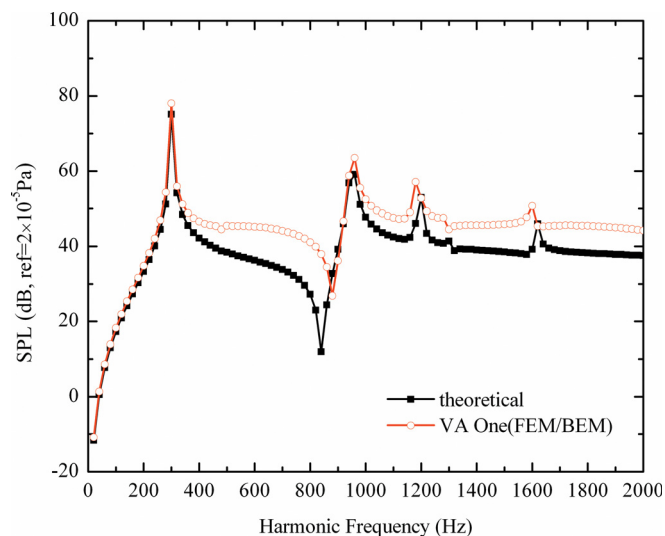


FIG. 13. (Color online) A comparison for the sound pressure level at 0.37% moisture content.

bit larger than the theoretical solution at medium and high frequencies. However, the overall dynamic characters of the theoretical results are in good agreement with the numerical result.

Figure 13 shows a comparison of the sound pressure level of the plate at 0.37% moisture content between the theoretical and numerical solutions. It is obvious in the plot that results obtained from VA ONE are fitted preferably with theoretical solutions in the whole frequency domain, especially at low frequencies. According to the Rayleigh integral Eq. (21), the sound pressure is influenced by the velocity of the plate, so the curve of numerical result is a little larger than the theoretical solution at medium and high frequencies, as expected.

V. CONCLUSIONS

The effect of the hygroscopic environment on the vibration response and consequent acoustic radiation of an orthotropic composite laminated plate is investigated. An analytic method is employed to carry out the critical buckling moisture content, vibration, and acoustic response. The average mean square velocity, sound pressure level, and radiation efficiency are computed for the simply supported boundary condition to show the effect of the elevated moisture loading on the vibration response and acoustic radiation. The vibration response and consequent acoustic radiation with different ratios of longitudinal Young's modulus to transverse Young's modulus are calculated and compared to research the effects of different stiffness values of the orthotropic plate in moisture load on the vibration and acoustic radiation characteristics. To verify the theoretical results, numerical simulations are carried out with commercial finite element software.

From the analysis of vibration characteristics, it can be found that the natural frequencies decrease with the increase of the moisture content and the first two order modes interconvert at high moisture content. There are peaks in each resonance frequency for average mean square velocity which moves to low frequencies with the elevated uniform moisture content applied on the plate as the stiffness reduces. Influenced by the dynamic response, the sound pressure level peaks also have a shift to lower frequency. The sound radiation efficiency generally floats to the low frequencies and decreases in the low and medium frequency band with the moisture content.

In the research of the effects for different stiffness values on the vibration and acoustic responses of the plate at moisture content, the peaks of resonance modes for dynamic response reduce with the enhancement of the stiffness due to the decreased ratio of longitudinal Young's modulus to the transverse modulus. And the numbers of peaks for sound pressure level which is influenced by the dynamic response also reduce in frequency band. The coincidence frequency decreases with the enhancement of the stiffness, and when the orthotropic plate is approximately equivalent to an isotropic plate, the plot of radiation efficiency shows a clear peak around the coincidence frequency, followed by an asymptotic reduction to unity, as expected.

In the validation study, the theoretical values and the numerical results generally match well. The error of the natural frequency for the (1, 2) mode, which is very sensitive to hygroscopic loads, is larger than others under hygroscopic environments. But the dynamic and acoustic responses show a good agreement between the theoretical and numerical results.

ACKNOWLEDGEMENTS

This work is supported by the National Natural Science Foundation of China (Grant No. 91016008 and 91216107).

- ¹S. M. Dickinson, "Lateral vibration of rectangular plates subject to in-plane forces," *J. Sound. Vib.* **16**, 465–472 (1971).
- ²S. R. Soni and C. L. Amba Rao, "Vibrations of orthotropic rectangular plates under in-plane forces," *Comput. Struct.* **4**, 1105–1115 (1974).
- ³Qing Hua Qin and T. J. Wang, "A theoretical analysis of the dynamic response of metallic sandwich beam under impulsive loading," *Eur. J. Mech A/Solids*. **28**, 1014–1025 (2009).
- ⁴Qing Hua Qin and T. J. Wang, "Low-velocity heavy-mass impact response of slender metal foam core sandwich beam," *Compos. Struct.* **93**, 1526–1537 (2011).
- ⁵Alain Berry, Jean-Louis Guyader, and Jean Nicolas, "A general formulation for the sound radiation from rectangular, baffled plates with arbitrary boundary conditions," *J. Acoust. Soc. Am.* **88**, 2792–2802 (1990).
- ⁶H. Nelisse, O. Beslin, and J. Nicolas, "A generalized approach for the acoustic radiation from a baffled or unbaffled plate with arbitrary boundary conditions, immersed in a light or heavy fluid," *J. Sound. Vib.* **211**, 207–225 (1998).
- ⁷P. Jeyaraj and Chandramouli Padmanabhan, "Vibration and acoustic response of an isotropic plate in a thermal environment," *Trans. ASME, J. Vib. Acoust.* **130**, 051005–051006 (2008).
- ⁸P. Jeyaraj, N. Ganesan, and Chandramouli Padmanabhan, "Vibration and acoustic response of a composite plate with inherent material damping in a thermal environment," *J. Sound. Vib.* **320**, 322–338 (2009).
- ⁹L. Shuyu, "Study on the radiation acoustic field of rectangular radiators in flexural vibration," *J. Sound. Vib.* **254**, 469–479 (2002).
- ¹⁰Chi-Moon Won, Kyong-Ku Yun, and Joo-Hyung Lee, "A simple but exact method for vibration analysis of composite laminated plates with all edges simply supported and under lateral and in-plane loading," *Thin-Walled Struct.* **44**, 247–253 (2006).
- ¹¹K. S. Sai Ram and P. K. Sinha, "Hygrothermal effects on the free vibration of laminated composite plates," *J. Sound. Vib.* **158**, 133–148 (1992).
- ¹²P. K. Parhi, S. K. Bhattacharyya, and P. K. Sinha, "Hygrothermal effects on the dynamic behavior of multiple delaminated composite plates and shells," *J. Sound. Vib.* **248**, 195–214 (2001).
- ¹³N. V. S. Naidu and P. K. Sinha, "Nonlinear finite element analysis of laminated composite shells in hygrothermal environments," *J. Compos. Struct.* **69**, 387–395 (2005).
- ¹⁴N. V. Swamy Naidu and P. K. Sinha, "Nonlinear transient analysis of laminated composite shells in hygrothermal environments," *J. Compos. Struct.* **72**, 280–288 (2006).
- ¹⁵N. V. Swamy Naidu and P. K. Sinha, "Nonlinear free vibration analysis of laminated composite shells in hygrothermal environments," *J. Compos. Struct.* **77**, 475–483 (2007).
- ¹⁶Constantinos S. Lyrantzis and Dimitri A. Bofilios, "Hygrothermal effects on structure-borne noise transmission of stiffened laminated composite plates," *J. Aircraft* **27**, 722–730 (1990).
- ¹⁷Qian Geng and Yueming Li, "Analysis of dynamic and acoustic radiation characters for a flat plate under thermal environments," *Int. J. Appl. Mech.* **4**, 1250028 (2012).
- ¹⁸S. Timoshenko and J. N. Goodier, *Theory of Elasticity* (McGraw-Hill, New York, 1951), Chap. 1, pp. 1–10.
- ¹⁹Autar K. Kaw, *Mechanics of Composite Materials* (Taylor & Francis, Boca Raton, 2006), Chap. 2, pp. 61–202.
- ²⁰Frank Fahy and Paolo Gardonio, *Sound and Structural Vibration: Radiation, Transmission and Response* (Elsevier Academic, Amsterdam, 2007), Chap. 3, pp. 135–241.
- ²¹M. Ohlrich and C. T. Hugin, "On the influence of boundary constraints and angle baffle arrangements on sound radiation from rectangular plates," *J. Sound. Vib.* **277**, 405–418 (2004).